Journal of
Ceramic Science
and Technology

J. Ceram. Sci. Tech., 02 [01] 69-74 (2011)
DOI: 10.4416/JCST2010-00038
available online at: http://www.ceramic-science.com

Microstructure and Mechanical Properties of Hot-Pressed Alumina – 5 vol% Zirconia Nanocomposites

F. Kern

Institute for Manufacturing Technologies of Ceramic Components and Composites, University of Stuttgart, D-70569 Stuttgart, Allmandring 7b

received October 8, 2010; received in revised form October 16, 2010; accepted October 22, 2010

Abstract

Zirconia-toughened alumina (ZTA) ceramics are known to combine the hardness and abrasion resistance of alumina with an additional toughness increment introduced by zirconia. Toughening occurs by transformation toughening and/or microcracking depending on the grain size and stabilizer content of zirconia. In this study ZTA with 5 vol% unstabilized nanozirconia was manufactured by means of a mixing and milling technique and consolidated by hot pressing at 1350 – 1600 °C. Variation of the sintering conditions leads to nanocomposites with different microstructural features, such as grain sizes and inter- or intragranular location of zirconia reinforcement. It was found that despite the low zirconia content, attractive hardness and strength levels as well as moderate toughness values can be obtained.

Keywords: Nanocomposites, ZTA, sintering, microstructure, zirconia, alumina

I. Introduction

ZTA materials with a zirconia reinforcement of up to 25 vol% in an alumina matrix have been widely used in the last 20 years for cutting tools, tribocomponents and other engineering applications requiring high hardness strength and toughness. Recently ZTAs have attracted considerable interest in biomedical applications owing to their higher aging resistance compared to Y-TZP [1,2].

From the viewpoint of toughening effects, ZTA may be subdivided into two main groups. Transformation-toughened ZTAs have a fine-grained (< 0.5 µm) tetragonal zirconia reinforcement that performs stress-induced martensitic phase transformation [3]. ZTA reinforced with unstabilized large-size zirconia grains (> 2 µm) forms monoclinic phase after cooling. This is accompanied by the formation of microcracks which provide additional toughness [4]. The transformability of the zirconia inclusions can be triggered by the amount of zirconia added and by the yttria stabilizer content. At low zirconia content up to 5 – 7 vol%, no stabilizer is required to keep the dispersion tetragonal provided that the zirconia grains are small and well dispersed [5]. In real ZTA materials toughening increments with both microcracking and transformation may contribute to the overall toughness.

Nanocomposite ZTA is not an invention of the nanomaterials hype of the recent years. In fact some of the first experiments on ZTA were conducted with co-precipitated alumina/zirconia powders derived from salt mixtures. These highly dispersed systems can lead to nanoscale zirconia inclusions in alumina grains after sintering [6]. Owing to cost reasons this manufacturing route was abandoned. ZTA nowadays is produced from mixing and milling of commercially available fine powders, this approach favours the location of zirconia in intergranular positions. Chevalier et al. have recently reported on ZTA materials with intragranular zirconia inclusions [7]. They used zirconia-coated sub-µm alumina coated with low amounts (~2 vol%) of zirconia. The resulting ZTA with large alumina grains and nanoscale intragranular zirconia inclusions leads to a material without R-curve behaviour and a high threshold toughness K_0 of 5 MPa · $\sqrt{m}$. The high toughness in these materials originated from neither of the classical mechanisms but from compressive stress of the inclusions on the surrounding alumina matrix. These characteristics make the materials interesting for components with cyclic loading. Homogeneous dispersion of zirconia to alumina by powder coating has been shown to improve the homogeneity and mechanical properties of ZTA [8,9]. Procedures proposed are, however, still very complicated; a suitable manufacturing scale-up has not yet been demonstrated. Earlier findings of the authors show that extremely fine-grained and fully dense ZTA materials can be processed by injection moulding and pressureless two-step sintering at temperatures as low as 1350 – 1375 °C [10]. Perfectly dispersed nanosize zirconia is extremely efficient in inhibiting grain growth of alumina. Resulting ZTA nanocomposites are extremely hard and abrasion resistant, toughness, however, is low because the zirconia grains are too small and the R-curve behaviour of ultrafine grain alumina is negligible. Applying Lange's formalism to the low-alloyed ZTAs leads to the conclusion that the transformation-related toughness increment added to the

* Corresponding author: frank.kern@ifkb.uni-stuttgart.de

toughness of pure alumina is $< 0.4\,\mathrm{MPa} \cdot \sqrt{\mathrm{m}}$ at 5 vol% zirconia addition [5]. The present study aims at quantifying the correlations between heat treatment conditions, resulting microstructures and corresponding mechanical properties of ZTA nanocomposites with small amounts of monoclinic zirconia. Hot pressing was chosen as a suitable manufacturing technology owing to the wider range of sintering temperatures and microstructural diversity of fully dense materials accessible.

II. Experimental

Ultrafine α-alumina (TM-DAR, Taimicron Japan) $d_{50} = 100 \pm 20$ nm, $S_{BET} = 14 \pm 1\,m^2/g$ was mixed with 5 vol% of pure zirconia nanopowder, $S_{BET}^* = 60 \pm 15\,m^2/g$, highly agglomerated, primary particle size $d_{50}^* = 12$ nm (*manufacturer's data, VP-PH, Evonik Germany). This zirconia nanopowder is an unstabilized nanopowder manufactured by means of flame pyrolysis, which is not entirely monoclinic in as-manufactured state owing to quenched tetragonal phase but becomes monoclinic on annealing at 800 °C [11]. A 300 g batch of blended powder was ball-milled in 500 ml 2-propanol with 3Y-TZP milling balls (d = 5 mm) in a polyethylene bottle for 24 h. After separating the milling balls, the solvent was evaporated at 85 °C. The resulting dry, weakly agglomerated powder was screened through a 200 µm mesh and dried at 130 °C to remove adsorbed solvent prior to pressing. The powders were hot-pressed in boron-nitride-clad graphite dies (d = 40 mm) in vacuum (KCE, Germany). Two disks of 11.5 g each were pressed at each temperature (1350 – 1600 °C, 50 K increments). Heating to final temperature was conducted at 50 K/min at a pre-load of 2 MPa, the pressing force of 60 MPa was applied upon reaching final temperature and kept during the dwell of 1 h. Cooling to room temperature was performed in the press at 1 bar argon atmosphere by switching off the heater.

The resulting disks were machined by lapping with 15 µm diamond suspension and subsequently polished with 6 µm and 3 µm diamond suspension for 1 h each (Struers Rotopol, Germany). Test bars of 4 mm width and ~2 mm thickness were cut with a diamond wheel (Struers, Germany). The edges and sides of the as-cut bars were carefully bevelled and polished with 15-µm diamond suspension to remove edge defects. Mechanical testing (10 samples each) was conducted by means of 4-pt bending with a span of 20 mm (Zwick, Germany). Vickers hardness HV_{10} (Bareiss, Germany) and microhardness $HV_{0.1}$ (Fischerscope , Germany) were measured. The indentation modulus was calculated from the microhardness measurement according to the universal hardness method. Indentation toughness values K_{IND} according to Anstis and Niihara (using the median crack model as c/a = 3.1 - 3.8) was calculated from the indent sizes, wing crack lengths and the indentation modulus [12, 13]. As indentation-based toughness determinations have recently been generally criticized, toughness measurements were validated with conservative indentation strength in bending (ISB) tests according to Chantikul [14, 15]. Phase compositions were determined by means of XRD on polished surfaces (Bruker D8, Germany) using the calibration curve according to Toraya [16]. Determination of the transformability of the dispersed zirconia by XRD of the fractured faces failed because the small signal strength was too small and the surfaces uneven. The microstructures of polished and thermally etched surfaces (1300 °C/1 h, air) were investigated by means of SEM at 5000x up to 20000x magnification (Jeol, Japan). Grain sizes were determined by means of the line intercept method according to Mendolson [17]. Independently, the trend in grain sizes of zirconia was determined from XRD data according to the Scherrer formula, the shift of the location of the tetragonal zirconia (101) reflex also yielded information on the residual stresses in the samples sintered at different final temperatures [18]. To avoid influence of shifting of the zero point of the 2θ-scale in the diffractometer with time, all samples were measured in one session. Density was determined with the Archimedes method.

III. Results and Discussion

(1) Mechanical properties

Vickers hardness and indentation modulus first show a clear and parallel trend to decline with rising sintering temperatures (Fig. 1). According to the Hall-Petch relationship, this behaviour was expected as the grain sizes increase with rising sintering temperatures. This trend is intact from 1350 – 1550 °C then at 1600 °C sintering temperature hardness and stiffness rise again considerably to the level measured at 1450 – 1500 °C. This unexpected result will be discussed in conjunction with the microstructural features. Fig. 2 shows the fracture toughness vs. sintering temperature. Fracture toughness values show a trend to increase with rising sintering temperatures. There are, however, distinct differences between the absolute values. The Niihara model seems to be overly optimistic. Comparing the ISB and Anstis models, which were originally calibrated against each other, it is surprising that the Anstis model seems to be slightly too conservative assuming that the residual strength method ISB model delivers "correct" values. At 1600 °C sintering temperature the toughness according to ISB falls while the toughness according Anstis rises further. This may hint at a different reaction of the two different approaches to changes in the reinforcement mechanisms.

Fig. 3 shows the 4-pt bending strength and the residual strength (ISB) after pre-damaging with a HV_{10} indent. From 1350 – 1500 °C sintering temperature, both curves follow the same trend while the relationship is inverse for the samples sintered at 1550 °C and 1600 °C. Bending strength rises from 590 to 670 MPa at a sintering temperature of 1500 °C, drops to 560 MPa at 1550 °C and rises again to 630 MPa at 1600 °C.

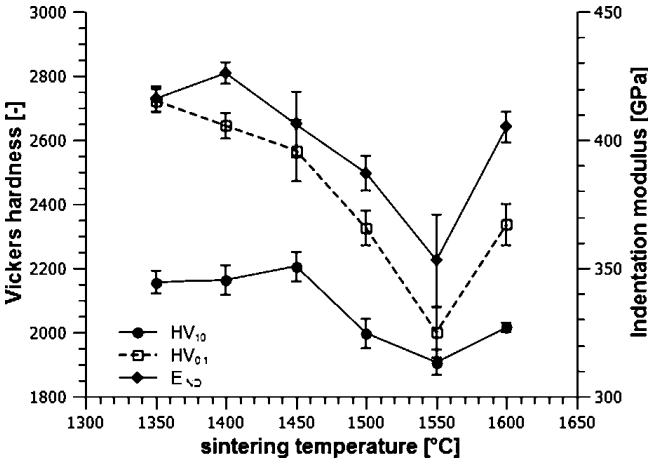

Fig. 1: Vickers hardness HV_{10} and $HV_{0.1}$ and indentation modulus E_{IND} vs. sintering temperature.

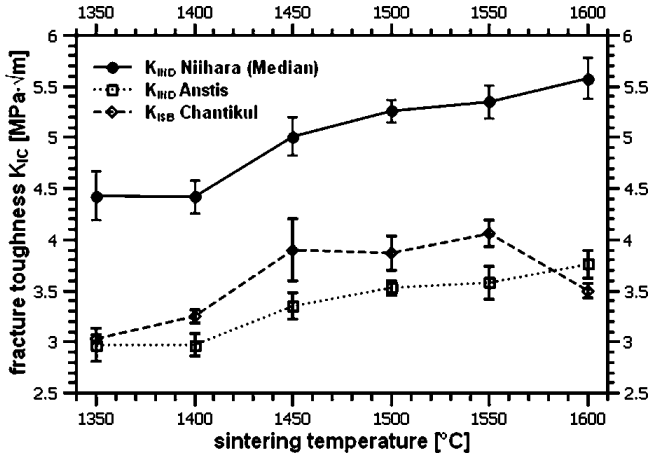

Fig. 2: Fracture toughness determined by the indentation (Anstis and Niihara) and ISB method (Chantikul) vs. sintering temperature.

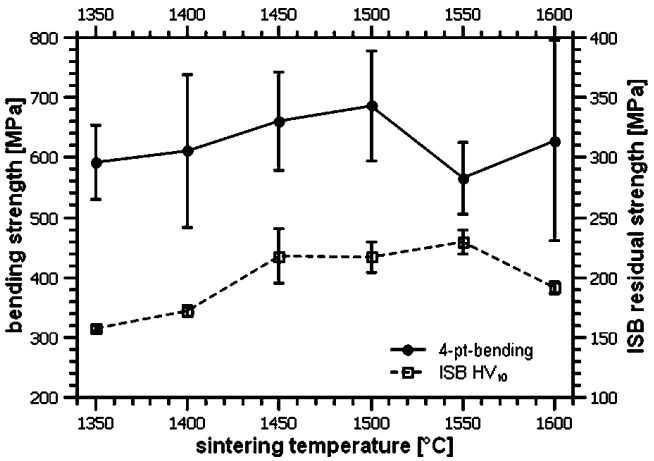

Fig. 3: 4-pt bending strength and residual strength after pre-damaging with a HV10 indent vs. sintering temperature.

Assuming full density and processing-specific identical flaw size and applying the Griffith criterion, a linear dependency between strength and toughness should be expected; this is, however, only true for the sintering temperatures up to 1500 °C. The toughness measurement as such does not reveal the origin of toughness, in ZTA the two main contributing mechanisms are transformation toughening and microcracking. In case of low zirconia content, a third contribution by residual stress may have to be considered [7]. To find out more on the reasons causing this deviation from expected values, the phase composition of the materials in polished condition was determined by means of XRD.

(2) Phase analysis

Fig. 4 shows the monoclinic content of the ZTA materials vs. sintering temperature. At low sintering temperatures 1350 °C – 1500 °C the monoclinic fraction is almost constant at 12 vol%. It has to be mentioned that owing to the low zirconia contents the standard deviations of the measured values are relatively high. At 1550 °C an abrupt rise in monoclinic content is observed. Owing to this increased monoclinic fraction, it can be assumed that in this case a considerable fraction of toughening is contributed by microcracking. This shift between mechanisms can be made responsible for the decrease in strength as we may expect that the formation of microcracks is detrimental to strength. At 1600 °C the monoclinic content declines again, which is associated with a rise in strength. The correctness of this explanation has to be validated by the results of the microstructural analysis.

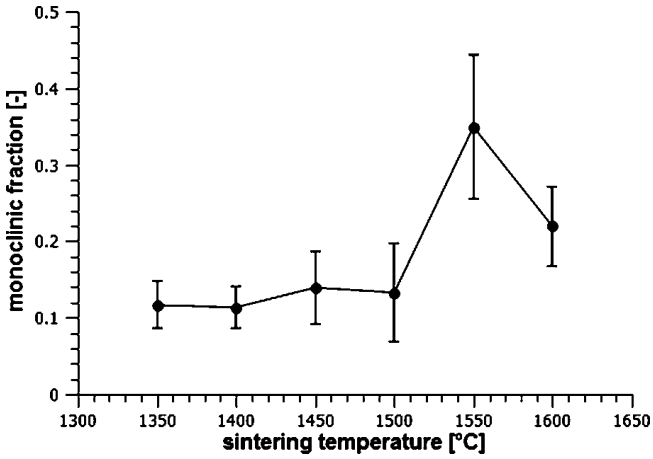

Fig. 4: Monoclinic content in polished surface of ZTA materials vs. sintering temperature.

XRD can further contribute to solving the discrepancies detected. Fig. 5 shows the calculated diameter of zirconia grains from line broadening (Scherrer analysis). Although the method is not suitable for determining correct absolute values of zirconia grain sizes in an alumina matrix, the trend and shape of the curve can help understanding of the nonlinearity of strength and toughness. In principle the diameter of a particle can be determined according to Scherrer's law. The particle size is inversely proportional to the line width of the XRD reflexes. The line broadening in a free-standing particle is dependent on its size (the number of lattice planes interacting with the XRD radiation) and a certain contribution by the diffractometer. The particle sizes determinable with a diffractometer are in the range between 10 – 50 nm. In our case the particles are in a matrix and considerably larger, thus no absolute values can be determined and the data are further influenced by stress introduced by cooling of the composite consisting of two materials with different CTE from sintering to ambient temperature. Stress can be uniform resulting in a shifting

of the peak to lower 2θ-values or non-uniform resulting in an additional line broadening. This additional broadening is responsible for the systematically too low size values. In good agreement with the theory, the location of the (101) reflex of tetragonal zirconia is shifted to lower angles with rising sintering temperatures owing to a rise in tensile stress on the zirconia particles, for a quantitative interpretation of stress the zirconia reflexes at higher 2θ-values should be checked. Again between 1550 and 1600 °C a discontinuity can be observed, which must be related to a structural change causing a partial release of stress. The declining apparent diameters between 1350 – 1450 °C are probably caused by a non-uniform stress which may be related to machining. Based on these results it was suspected that the stress-release mechanism is related to the coarsening of the alumina matrix at high sintering temperatures and coalescence of small grains as well as with the incorporation of zirconia into the alumina grains. The results of microstructure analysis revealed that the effects are more complex.

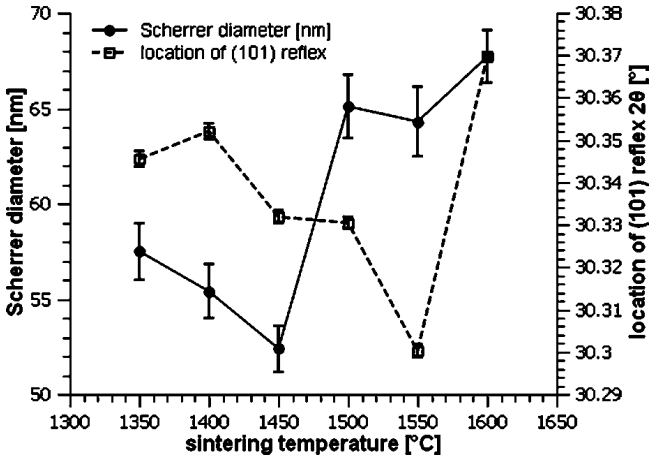

Fig. 5: Mean zirconia particle diameter in ZTA composite calculated from line broadening and shift of tetragonal (101) reflex vs. sintering temperature.

(3) Microstructural characterization

Evidence for the statements made before – more or less *a priori* – can be found in the following SEM images (Figs. 6 - 9). Samples sintered at 1350 °C (Fig. 6) show a fine-grained microstructure (grain sizes 0.5 – 1 µm) in the regions where zirconia is present. In zirconia-free regions (lower right) the grains are much larger, reaching sizes of 3 – 4 µm. Zirconia is located exclusively in an intergranular position. These microstructural features are retained in samples fired at 1400 °C (not shown). Further increase of the sintering temperature leads to considerable grain growth, at 1450 °C (Fig. 7), only few small alumina grains are left. Zirconia grains of larger size (> 0.3 µm) stay at grain boundaries, smaller grains are "swallowed" by the growing alumina grains. While intergranular zirconia grains stay faceted, intragranular zirconia grains are perfectly globular. The breakdown of the inter-type microstructure was expected as Lange and Hirlinger have shown that 5 vol% zirconia is not sufficient to occupy all four junctions of alumina grains and thus to permanently prevent alumina grain growth in ZTA [19]. Increasing the sintering temperature further amplifies this tendency. Fig. 8 shows that at 1550 °C the alumina grains grow to 4 – 5 µm diameter. The size of intergranular zirconia grains seems to increase while the size of intragranular grains stays unaffected. One would expect that at higher sintering temperature this tendency to further coarsen-

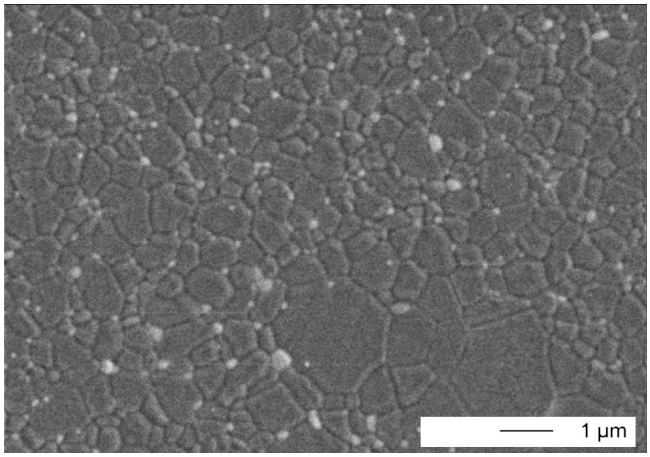

Fig. 6: Microstructure of ZTA sintered at 1350 °C/1 h/50 MPa, thermally etched surface (1300 °C/30 min, air)

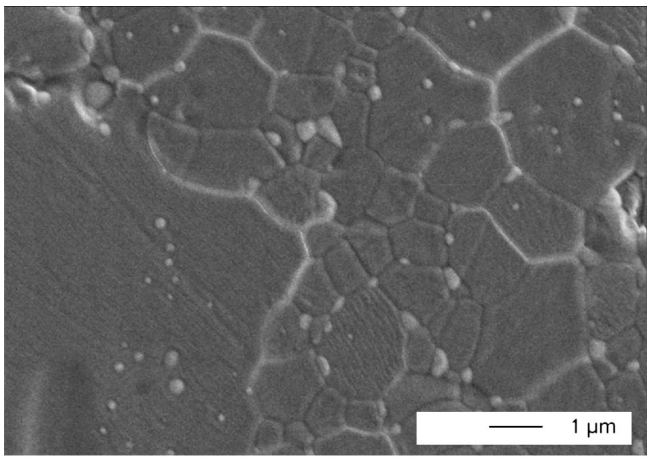

Fig. 7: Microstructure of ZTA sintered at 1450 °C/1 h/50 MPa, thermally etched surface (1300 °C/30 min, air).

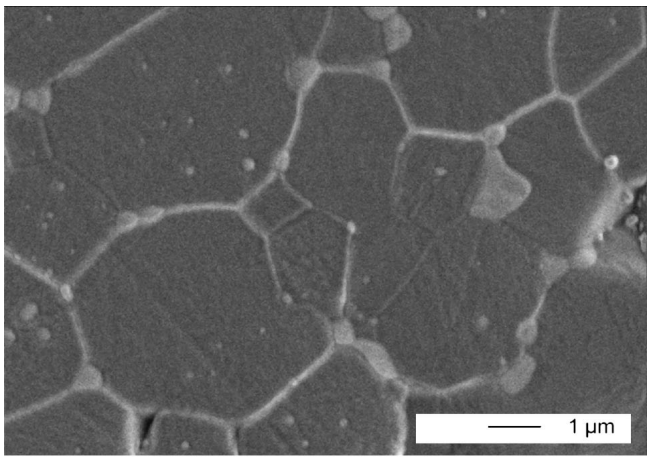

Fig. 8: Microstructure of ZTA sintered at 1550 °C/1 h/50 MPa, thermally etched surface (1300 °C/30 min, air).

ing should proceed. However, at 1600 °C (Fig. 9) an unexpected reduction in alumina matrix grain sizes is observed. More intergranular zirconia of small size can be detected. To check if this effect was real or just an artefact of a random choice of the high-magnification image, SEM images of lower magnification were inspected. The presence of the grain refinement effect was confirmed. Large alumina grains were only detected in such regions free of zirconia.

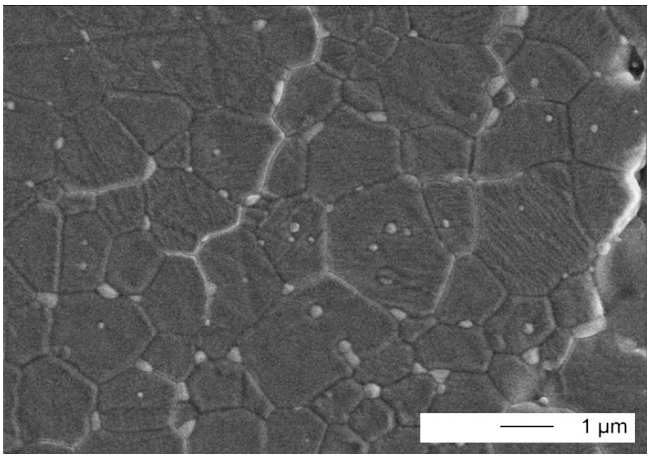

Fig. 9: Microstructure of ZTA sintered at 1600 °C/1 h/50 MPa, thermally etched surface (1300 °C/30 min, air).

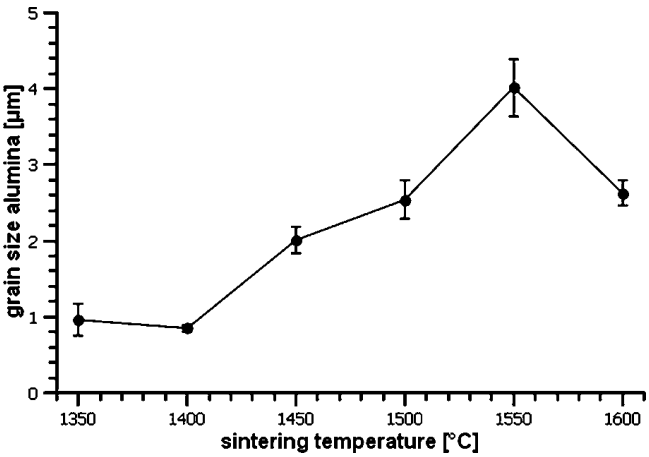

Fig. 10: Grain sizes of alumina in ZTA composites at different temperatures determined according to Mendelson with the line intercept method.

Taking into account the observations made during determination of mechanical properties and the results of phase analysis, a conclusive interpretation can be made. The stress generated during cooling from sintering temperature increases with rising sintering temperatures. As soon as the compressive stress on the alumina matrix exceeds a critical limit, the matrix grains begin to recrystallize during cooling from sintering temperature. The clearly visible cracks in the samples fired at 1450 – 1550 °C which were not present in the polished samples and originate during thermal etching further support this interpretation. At 1600 °C, fewer cracks were detected. Large intergranular grains of zirconia, which turn monoclinic during cooling, may also contribute to this grain refinement. One may suspect that the formation of new grain boundaries may result from twinning of the alumina grains, a detailed explanation cannot yet be given. The formation of new grain boundaries seems to be the mechanism by which the cooling stress is finally accommodated. Niihara suggested a similar explanation for the improved toughness and strength after annealing of alumina-SiC, the comparison is, however, not perfectly sound as in alumina-SiC the stresses in matrix and dispersion are inverse compared to ZTA. An overview of the evolution of alumina matrix grain sizes is shown in Fig. 10. Grain sizes of zirconia can only be estimated from the SEM images.

IV. Summary

ZTA nanocomposites with 5 vol% monoclinic nanosize zirconia reinforcement were produced by hot pressing. The materials show high hardness and mechanical strength at a moderate toughness level. The low fraction of zirconia is only capable of keeping the microstructure fine-grained at low sintering temperatures. At 1350 – 1400 °C, an intertype nanocomposite structure prevails. At higher sintering temperatures more zirconia is entrapped in larger alumina grains, only large zirconia grains stay at the grain boundaries. An intra-inter composite is formed. This breakdown of the initial microstructure was expected. Zirconia inclusions cause cooling stress owing to their higher CTE. At 1550 °C this stress obviously becomes critical; this statement is supported by the minima in hardness, indentation modulus and strength as well as the maximum in monoclinic content. Between 1550 – 1600 °C the piled-up stress finally leads to unexpected grain refinement, which acts as a mechanism for stress release. This effect may be specific to hot pressing as here densification takes place almost exclusively at final sintering temperature so that the cooling stress is higher than in pressurelessly sintered samples.

The effects observed in hot-pressed materials deserve further investigation e.g. by means of transmission electron microscopy or high-resolution XRD, which were unavailable for this study. Furthermore the effects should be monitored with respect to different initial grain sizes of alumina and zirconia powders as well as for pressureless sintering.

References

1 Deville, S., Chevalier, J., Fantozzi, G., Bartolomé, J.F., Requena, J., Moya, J.S., Torrecillas, R., Díaz, L.A.: Development of Advanced Zirconia-Toughened Alumina Nanocomposites for Orthopaedic Applications, *Key Engineering Materials*, 264-268, 2013-2016, (2004).

2 Chevalier, J., Grandjean, S., Kuntz, M., Pezzotti, G..: On the kinetics and impact of tetragonal to monoclinic transformation in an alumina/zirconia composite for arthroplasty applications, *Biomaterials*, **30** [9], 5279-5282, (2009).

3 Becher, P., Swain, M.: Grain-Size-Dependent Transformation Behavior in Polycrystalline Tetragonal Zirconia, *J. Am. Ceram. Soc.*, **75** [3], 493-502, (1992).

4 Claussen, N.: Fracture Toughness of Al_2O_3 with an Unstabilized ZrO_2 Dispersed Phase, *J. Am. Ceram. Soc.*, **59** [1-2], 49-51, (1976).

5 Lange, F.F.: Transformation toughening, part 4: Fabrication, fracture toughness and strength of Al_2O_3 - ZrO_2 composites, *J. Mat. Sci.*, **17**, 247-254, (1982).

6 Heuer, A.H., Claussen, N., Kriven W.M., Rühle, M.: Stability of Tetragonal ZrO_2 Particles in Ceramic Matrices, *J. Am. Ceram. Soc.*, **65** [12], 642-650, (1982).

[7] Chevalier, J., Deville, S., Fantozzi, G., Bartolome, J.F., Pecharroman, C., Moya, J.S., Diaz, L.A., Torrecillas, R.: Nanostructured Ceramic Oxides with a Slow Crack Growth Resistance Close to Covalent Materials, *Nanoletters*, **5** [7], 1297-1301, (2005).

[8] Jia, Y., Hotta, Y., Sato, K., Watari, K.: Homogeneous ZrO_2-Al_2O_3 composite prepared by Nano-ZrO_2 particle multilayer coated Al_2O_3 particles, *J. Am. Ceram. Soc.*, **89** [3], 1103-1106, (2006).

[9] Palmero, P., Naglieri, V., Chevalier, J., Fantozzi, G., Montanaro, L.: Alumina-based nanocomposites obtained by doping with inorganic salt solutions: Application to immiscible and reactive systems, *J. Eur. Ceram. Soc.*, **29** [1], 59-66, (2009).

[10] Gadow, R., Kern, F.: Pressureless sintering of injection molded zirconia toughened alumina nanocomposites, *J. Cer. Soc. Jap.*, **114** [11], 958-962, (2006).

[11] Kern, F.: 2.5Y-TZP from yttria-coated pyrogenic zirconia nanopowder, *J. Cer. Sci. Tech.*, **1** [1], 21-26, (2010).

[12] Anstis, G.R., Chantikul, P., Lawn, B.R., Marshall, D.B.A.: A critical evaluation of indentation techniques for measuring fracture toughness. I. Direct crack measurements, *J. Am. Ceram. Soc.*, 64, 533-538, (1981).

[13] Niihara, K.: A fracture mechanics analysis of indentation-induced Palmqvist crack in ceramics, *J. Mat. Sci. Let.*, **2**, 221-223, (1983)

[14] Quinn G.D., Bradt R.C.: On the Vickers Indentation Fracture Toughness Test, J. *Am. Ceram. Soc.*, **90** [3], 673-680, (2007).

[15] Chantikul, P., Anstis, G.R., Lawn, B.R., Marshall, D.B.A.: A critical evaluation of indentation techniques for measuring fracture toughness. II. Strength method, *J. Am. Ceram. Soc.*, **64**, 539-543, (1981).

[16] Toraya, H., Yoshimura, M., Somiya, S.: Calibration Curve for Quantitative Analysis of the Monoclinic-Tetragonal ZrO_2 System by X-Ray Diffraction, *J. Am. Ceram. Soc.*, **67**, 6, C119-121, (1984).

[17] Mendelson, M.I.: Average grain size in polycrystalline ceramics, *J. Am. Ceram. Soc.*, **52**, 443, (1969).

[18] Patterson, A.L.: The Scherrer formula for X-Ray particle size determination, *Physical Review*, **56**, 978-982, (1939).

[19] Lange, F.F., Hirlinger, M.: Hindrance of Grain Growth in Al_2O_3 by ZrO_2 Inclusions, *J. Am. Ceram. Soc.*, **67** [3], 164-168, (1982).